Supplementary Material for Effects of multivariate recovery dependency on resilience and scaling laws in networks with time delays

Xun Zhou,[1,*] Fan Wang,[2,*] Ruijin Du,[1,†] Duxin Chen,[3,‡]

Hillel Sanhedrai,[4] Renaud Lambiotte,[1,5] and Gaogao Dong[1,2,§]

[1]*School of Mathematical Sciences, Jiangsu University, Zhenjiang 212013, China*

[2]*Ministry of Education Key Laboratory of NSLSCS,*

School of Mathematical Sciences, Nanjing Normal University, Nanjing 210023, China

[3]*School of Mathematics, Southeast University, Nanjing 211189, China*

[4]*Department of Physics, Bar-Ilan University, Ramat-Gan 52900, Israel*

[5]*Mathematical Institute, University of Oxford, Oxford OX2 6GG, UK*

[*]These authors contributed equally to this work.

[†]Corresponding author: mathdudo@ujs.edu.cn

[‡]Corresponding author: chendx@seu.edu.cn

[§]Corresponding author: gago999@126.com

Appendix A: Parameters involved in this paper

The model parameters are summarized in Table A1.

TABLE A1: Parameters involved in the model

Symbol	Description
N	Network size
$\langle k \rangle$	The average degree of the ER network
$\widetilde{\lambda}$	The power-law exponent of the SF network
X, Y	The two specific layers of the network
μ	An arbitrary layer index, where $\mu \in \{X, Y\}$
t	Evolution time
τ	Time delay
$x_i(t)$, $y_i(t)$	Node state (0 indicates failure, 1 indicates normal operation)
$\langle x_i(t) \rangle$	The local state within the self-layer on which node i depends
$\langle y_i(t) \rangle$	The local state within the external-support layer on which node i depends
p	Initial failure fraction at $t = 0$
γ_μ^{d}	Failure rate in layer μ for $t > 0$
$\gamma_{\mu,\mathrm{inner}}^{\mathrm{r},0}$	Baseline recovery contribution for nodes in layer μ provided by the self-layer for $t \geq \tau$
$\gamma_{\mu,\mathrm{inter}}^{\mathrm{r},0}$	Baseline recovery contribution for nodes in layer μ provided by the external-support layer for $t \geq \tau$
$\gamma_\mu^{\mathrm{r},0}$	Baseline recovery rate of each node in layer μ for $t \geq \tau$
$k_{\mu,i}$	Degree of node i in layer μ
λ	Rate parameter in exponential distribution
α_1	Strength of the recovery dependency on the self-layer, with $\alpha_1 \in [0, 1]$
α_2	Strength of the recovery dependency on the external-support layer, with $\alpha_2 \in [0, 1]$
$\varphi(x)$	Function capturing the inner recovery dependencies within the self-layer
$\psi(x)$	Function capturing the inter recovery dependencies from the external-support layer
$f_\mu(t)$	Fraction of functional nodes in layer μ at time t
f_μ^*	The stabilized functional fraction in layer μ
$\overline{f_\mu^*}$	The average stabilized functional fraction in layer μ
P_{RS}	Probability of recovery success
T_{RS}	The average recovery time
γ, κ, ν	Scaling exponents

Appendix B: Modeling multivariate recovery dependency

The loss of resilience during extreme perturbations indicates that the hypothesis of a constant recovery rate is not sufficient to explain the system's behavior [1]. Given that the repair process depends on support from both the local system and external systems, we hypothesize that a multi-network approach could explain the observed deviation. Here, we formulate a time-dependent recovery rate. For $t \geq \tau$, we have

$$\gamma^{\mathrm{r}}_{X,i}(t) = g(\langle x_i(t)\rangle, \langle y_i(t)\rangle), \tag{B1}$$

where $g(\cdot)$ is an unknown function that represents the dependence of node i in network X on its own local environment and the environment of the corresponding node in network Y. The average state of node i is expressed as

$$\langle x_i(t)\rangle = \frac{1}{k_{X,i}} \sum_j X_{ij} x_j(t), \tag{B2}$$

and

$$\langle y_i(t)\rangle = \frac{1}{k_{Y,i}+1} \sum_j \widetilde{Y}_{ij} y_j(t), \tag{B3}$$

where X_{ij} and $\widetilde{Y}_{ij}$ are the adjacency matrices of the corresponding networks. These two quantities capture the evolving local state around node i in layer X and its recovery-dependent node in layer Y, respectively, indicating that the recovery resources are sourced from the vicinity of the failure. Note that in (B3), we use $\widetilde{Y}_{ij} = Y_{ij} + I_{ij}$ instead of Y_{ij}, where I_{ij} represents the element of the identity matrix. Since the recovery function can be identically rewritten using the natural logarithm as $g(\cdot) = \exp[\ln g(\cdot)]$, we obtain

$$\gamma^{\mathrm{r}}_{X,i}(t) = \exp\left[\ln g(\langle x_i(t)\rangle, \langle y_i(t)\rangle)\right]. \tag{B4}$$

Performing a first-order Taylor expansion with the Peano remainder on the logarithmic function inside the exponent around the fully functional state $(1,1)$, we have

$$\begin{aligned} \ln g(\langle x_i(t)\rangle, \langle y_i(t)\rangle) = \ln g(1,1) &+ \frac{g_x(1,1)}{g(1,1)}(\langle x_i(t)\rangle - 1) \\ &+ \frac{g_y(1,1)}{g(1,1)}(\langle y_i(t)\rangle - 1) + o(\rho), \end{aligned} \tag{B5}$$

where $g_x(1,1) \equiv \frac{\partial g}{\partial \langle x_i\rangle}\big|_{(1,1)}$ and $g_y(1,1) \equiv \frac{\partial g}{\partial \langle y_i\rangle}\big|_{(1,1)}$ denote the partial derivatives evaluated at $(1,1)$, and $\rho = \sqrt{(\langle x_i(t)\rangle - 1)^2 + (\langle y_i(t)\rangle - 1)^2}$. Substituting this expansion back and neglecting

the higher-order infinitesimal term $o(\rho)$ under the linear approximation, the recovery rate becomes

$$\gamma^{\mathrm{r}}_{X,i}(t) = \exp\left[\ln g(1,1) - \frac{g_x(1,1)}{g(1,1)}(1-\langle x_i(t)\rangle) - \frac{g_y(1,1)}{g(1,1)}(1-\langle y_i(t)\rangle)\right], \tag{B6}$$

which naturally separates into a product of exponential factors

$$\gamma^{\mathrm{r}}_{X,i}(t) = g(1,1)\cdot\exp\left[-\frac{g_x(1,1)}{g(1,1)}(1-\langle x_i(t)\rangle)\right]\cdot\exp\left[-\frac{g_y(1,1)}{g(1,1)}(1-\langle y_i(t)\rangle)\right]. \tag{B7}$$

To capture the leading-order behavior, we apply the first-order approximation $\exp(-z)\approx 1-z$ to the separated exponential terms, arriving at the decoupled form

$$\gamma^{\mathrm{r}}_{X,i}(t) = g(1,1)\left[1-\frac{g_x(1,1)}{g(1,1)}(1-\langle x_i(t)\rangle)\right]\left[1-\frac{g_y(1,1)}{g(1,1)}(1-\langle y_i(t)\rangle)\right]. \tag{B8}$$

Denoting with $\gamma^{\mathrm{r},0}_X = g(1,1)$ the baseline recovery rate and with $\alpha_1 = \frac{g_x(1,1)}{g(1,1)}$, $\alpha_2 = \frac{g_y(1,1)}{g(1,1)}$, we obtain

$$\gamma^{\mathrm{r}}_{X,i}(t) = \gamma^{\mathrm{r},0}_X\left[1-\alpha_1(1-\langle x_i(t)\rangle)\right]\left[1-\alpha_2(1-\langle y_i(t)\rangle)\right]. \tag{B9}$$

This derivation enables us to describe the expected behavior of $g(\cdot)$ to first order. We assume that $\alpha_j\in[0,1]$ for $j\in\{1,2\}$. Specifically, we assume that damage in one layer will not improve the repair of the other ($g_x(1,1)\geq 0\Rightarrow\alpha_1\geq 0$, $g_y(1,1)\geq 0\Rightarrow\alpha_2\geq 0$) and that the recovery rate must remain nonnegative ($|g_x(1,1)|\leq|g(1,1)|\Rightarrow\alpha_1\leq 1$, $|g_y(1,1)|\leq|g(1,1)|\Rightarrow\alpha_2\leq 1$).

To intuitively capture the joint dependence effect of internal and external repairs, the time-dependent recovery rate for $t\geq\tau$ can be expressed as

$$\gamma^{\mathrm{r}}_{X,i}(t) = \gamma^{\mathrm{r},0}_{X,\mathrm{inner}}\gamma^{\mathrm{r},0}_{X,\mathrm{inter}}\varphi(\langle x_i(t)\rangle)\psi(\langle y_i(t)\rangle), \tag{B10}$$

where $\gamma^{\mathrm{r},0}_{X,\mathrm{inner}}$ and $\gamma^{\mathrm{r},0}_{X,\mathrm{inter}}$ represent the baseline recovery contributions obtained from the self-layer and the external-support layer, respectively. The constant $\gamma^{\mathrm{r},0}_X$ represents a fixed level of recovery, which is explicitly decomposed as

$$\gamma^{\mathrm{r},0}_X = \gamma^{\mathrm{r},0}_{X,\mathrm{inner}}\gamma^{\mathrm{r},0}_{X,\mathrm{inter}}. \tag{B11}$$

Furthermore, the functions φ and ψ characterize the linear dependencies on the evolving local states of the self-layer and the external-support layer, defined respectively as

$$\varphi(\langle x_i(t)\rangle) = 1-\alpha_1(1-\langle x_i(t)\rangle), \tag{B12}$$

and

$$\psi(\langle y_i(t)\rangle) = 1-\alpha_2(1-\langle y_i(t)\rangle). \tag{B13}$$

Appendix C: Fraction of functional nodes under time delay

The dynamic evolution of these states is modeled using discrete time steps $t = 0, 1, 2, \ldots$. Initially, all nodes are fully functional, and node failures occur in two stages. In Stage I (at $t = 0$), a fraction p of nodes in each network fails, representing an initial attack. In Stage II (for $t > 0$), each remaining functional node is subject to a failure rate γ_μ^{d} at each time step, representing subsequent random failures.

Therefore, the initial condition is given by $f_\mu(0) = 1 - p$. A time delay $\tau > 0$ implies that during the interval from $t = 1$ to $t = \tau - 1$, the nodes cannot be repaired, yielding $\gamma_{X,i}^{\mathrm{r}}(t) = 0$. However, the failure process governed by γ_μ^{d} continues. Consequently, the fraction of functional nodes follows the recurrence relation

$$f_\mu(t+1) - f_\mu(t) = -\gamma_\mu^{\mathrm{d}} f_\mu(t). \tag{C1}$$

The right side of (C1) represents the decrement of functional nodes, indicating that a proportion γ_μ^{d} of the currently functional nodes are damaged at each step. This linear difference equation has a standard geometric progression solution

$$f_\mu(t) = f_\mu(0)(1 - \gamma_\mu^{\mathrm{d}})^t. \tag{C2}$$

Substituting the initial condition $f_\mu(0) = 1 - p$ into (C2), we obtain

$$f_\mu(t) = (1 - p)(1 - \gamma_\mu^{\mathrm{d}})^t. \tag{C3}$$

For a sufficiently small discrete failure rate ($\gamma_\mu^{\mathrm{d}} \ll 1$), we can apply the asymptotic approximation $1 - x \approx \exp(-x)$ [2]. Using this approximation, the term $(1 - \gamma_\mu^{\mathrm{d}})$ can be expressed as $\exp(-\gamma_\mu^{\mathrm{d}})$. Thus, the discrete iterative process can be transformed into a continuous exponential decay form

$$f_\mu(t) = (1 - p)\exp(-\gamma_\mu^{\mathrm{d}} t). \tag{C4}$$

Appendix D: Calculation of the mean recovery and failure times

For each parameter set, I independent numerical simulations are performed. Each realization eventually reaches one of two steady states, corresponding to successful recovery or system failure. Accordingly, the total number of realizations can be written as

$$I = I_{\mathrm{S}} + I_{\mathrm{F}}, \tag{D1}$$

where I_{S} and I_{F} denote the numbers of successfully recovered and failed realizations, respectively. In the numerical simulations, a steady state is identified when the change in the functional fraction between successive time steps is smaller than a sufficiently small tolerance ε. The converged state is classified as successful recovery if the system reaches a functional state, and as system failure if it reaches the collapsed state.

For each successfully recovered realization, the recovery time is defined as the time at which the system first reaches the recovered steady state. The mean recovery time is then calculated as

$$T_{\mathrm{RS}} = \frac{1}{I_{\mathrm{S}}} \sum_{m=1}^{I_{\mathrm{S}}} t_{\mathrm{RS}}^{(m)}, \tag{D2}$$

where $t_{\mathrm{RS}}^{(m)}$ is the recovery time of the mth successfully recovered realization.

Similarly, for each failed realization, the failure time is defined as the time at which the system first reaches the failed steady state. The corresponding mean failure time is calculated as

$$T_{\mathrm{RF}} = \frac{1}{I_{\mathrm{F}}} \sum_{m=1}^{I_{\mathrm{F}}} t_{\mathrm{RF}}^{(m)}, \tag{D3}$$

where $t_{\mathrm{RF}}^{(m)}$ is the failure time of the mth failed realization.

Appendix E: Scaling behaviors in additional network topologies

The main text discusses coupled networks constructed from ER and SF networks. Here, we further consider stochastic block model (SBM) networks [3] and spatial hyperbolic networks [4, 5]. For SBM networks, nodes are organized into communities, with the parameter $\widetilde{\mu}$ controlling the extent of connections between different communities. For spatial hyperbolic networks, node connectivity depends on spatial distance in hyperbolic space, with the temperature parameter T controlling the strength of the spatial constraint. In both cases, the average degree is set to $\langle k \rangle = 4$.

SBM networks and spatial hyperbolic networks represent two typical network topologies with modular structures and spatial constraints, respectively. Figure E1 presents the two scaling behaviors in these networks. Figures E1(a) and (b) show the first scaling behavior for SBM and spatial hyperbolic networks, respectively, while Figures E1(c) and (d) show the second scaling behavior for the corresponding networks. Both scaling behaviors can be observed in these two types of networks, indicating that they are not limited to ER and SF networks and providing further support for their generality across different network topologies.

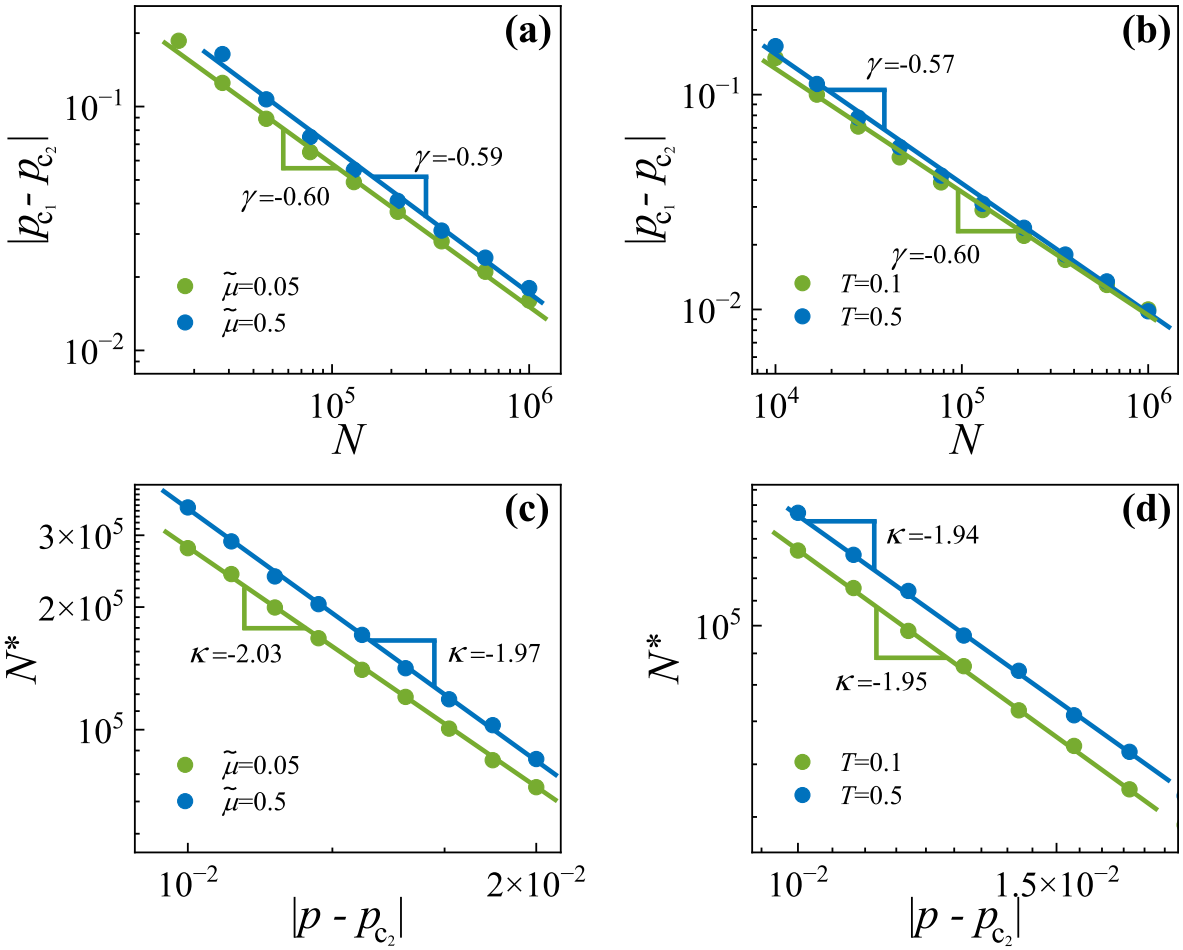

FIG. E1: Scaling behaviors in SBM and spatial hyperbolic networks. (a) and (c) Results for SBM networks with $\tilde{\mu} = 0.05$ and 0.5; (b) and (d) results for spatial hyperbolic networks with $T = 0.1$ and 0.5. (a) and (b) show $|p_{c_1} - p_{c_2}|$ as a function of network size N, whereas (c) and (d) show N^* as a function of $|p - p_{c_2}|$. Other parameters are $\langle k \rangle = 4$, $\gamma^{r,0}_{X,\text{inner}} = \gamma^{r,0}_{X,\text{inter}} = 0.8$, $\alpha_1 = \alpha_2 = 1$, and $\lambda = 0.01$.

Appendix References

[1] Danziger M M, Barabási A L. Recovery coupling in multilayer networks. Nat Commun, 2022, 13: 955

[2] Majdandzic A, Podobnik B, Buldyrev S V, et al. Spontaneous recovery in dynamical networks. Nat Phys, 2014, 10: 34–38

[3] Holland P W, Laskey K B, Leinhardt S. Stochastic blockmodels: First steps. Soc Networks, 1983, 5: 109–137

[4] Krioukov D, Papadopoulos F, Kitsak M, et al. Hyperbolic geometry of complex networks. Phys Rev E, 2010, 82: 036106

[5] Dettmann C P, Georgiou O. Random geometric graphs with general connection functions. Phys Rev E, 2016, 93: 032313